

---

# Sample-Efficient Optimization in the Latent Space of Deep Generative Models via Weighted Retraining

---

**Austin Tripp\***  
University of Cambridge  
ajt212@cam.ac.uk

**Erik Daxberger\***  
University of Cambridge  
Max Planck Institute for  
Intelligent Systems, Tübingen  
ead54@cam.ac.uk

**José Miguel Hernández-Lobato**  
University of Cambridge  
Alan Turing Institute  
Microsoft Research  
jmh233@cam.ac.uk

## Abstract

Many important problems in science and engineering, such as drug design, involve optimizing an expensive black-box objective function over a complex, high-dimensional, and structured input space. Although machine learning techniques have shown promise in solving such problems, existing approaches substantially lack sample efficiency. We introduce an improved method for efficient black-box optimization, which performs the optimization in the low-dimensional, continuous latent manifold learned by a deep generative model. In contrast to previous approaches, we actively steer the generative model to maintain a latent manifold that is highly useful for efficiently optimizing the objective. We achieve this by periodically *retraining* the generative model on the data points queried along the optimization trajectory, as well as *weighting* those data points according to their objective function value. This weighted retraining can be easily implemented on top of existing methods, and is empirically shown to significantly improve their efficiency and performance on synthetic and real-world optimization problems.

## 1 Introduction

Many important problems in science and engineering can be formulated as optimizing an objective function over an input space. Solving such problems becomes particularly challenging when 1) the input space is high-dimensional and/or *structured* (i.e. discrete spaces, or non-Euclidean spaces such as graphs, sequences, and sets) and 2) the objective function is expensive to evaluate. Unfortunately, many real-world problems of practical interest have these characteristics. A notable example is drug design, which has a graph-structured input space, and is evaluated using expensive wet-lab experiments or time-consuming simulations. Recently, machine learning has shown promising results in many problems that can be framed as optimization, such as conditional image [57, 40] and text [44] generation, molecular and materials design [11, 47], and neural architecture search [10]. Despite these successes, using machine learning on structured input spaces and with limited data is still an open research area, making the use of machine learning infeasible for many practical applications.

One promising approach which tackles *both* challenges is a two-stage procedure that has emerged over the past few years, which we will refer to as *latent space optimization (LSO)* [13, 29, 33, 34, 41]. In the first stage, a (deep) generative model is trained to map tensors in a low-dimensional continuous space onto the data manifold in input space, effectively constructing a low-dimensional and continuous analog of the optimization problem. In the second stage, the objective function is optimized over this learned latent space using a surrogate model. Despite many successful applications in a variety of fields including chemical design [13, 21, 29, 5] and automatic machine learning [33, 34], LSO is primarily applied in a *post-hoc* manner using a pre-trained, general purpose generative model rather

---

\*equal contribution

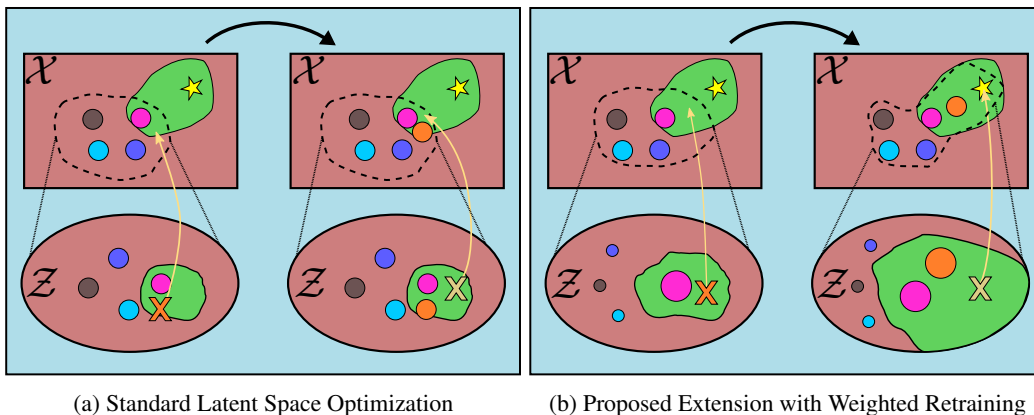


Figure 1: Schematic of two iterations of LSO with and without our proposed extension of weighted retraining of the generative model  $g : \mathcal{Z} \mapsto \mathcal{X}$ . **(a)** The standard approach keeps  $g$  (and thus the latent space  $\mathcal{Z}$ ) fixed throughout the optimization. It is only able to find points close to the training data used to learn  $\mathcal{Z}$ , resulting in slow and incomplete exploration of  $\mathcal{X}$ . **(b)** Our proposed approach weights data points according to their objective function value and retrains  $g$  to incorporate newly queried data. This continually adjusts  $\mathcal{Z}$  to focus on modelling the most promising regions of  $\mathcal{X}$ , speeding up the optimization and allowing for substantial extrapolation beyond the initial training data. **Symbols:** Red/green regions correspond to points with low/high objective function values, respectively. The yellow star is the global optimum in  $\mathcal{X}$ . Coloured circles are data points; their radius in  $\mathcal{Z}$  corresponds to their assigned weight. Crosses are queries made during optimization. The dashed line surrounds the region of  $\mathcal{X}$  modelled by  $g$  (i.e.  $g(\mathcal{Z})$ , the image of  $\mathcal{Z}$ ).

than one trained specifically for the explicit purpose of downstream optimization. Put differently, the training of the generative model is effectively *decoupled* from the optimization task.

In this paper, we identify and examine two types of decoupling in LSO, and argue that they both make optimization unnecessarily difficult, and fundamentally prevent LSO from finding solutions that lie far from the training data. Motivated by this, we then present *weighting of the data distribution* and *periodic retraining of the generative model* to effectively resolve this decoupling. We argue that these two proposed modifications are highly complementary, fundamentally transforming LSO from a local optimizer into an efficient global optimizer capable of recursive self-improvement. The core contributions of our paper are the following:

1. We identify and describe two critical failure modes of previous LSO-based methods which severely limit their efficiency and performance, and thus practical applicability (Section 3).
2. We propose to combine dataset weighting with periodic retraining of the generative model used within LSO as an effective way to directly address the issued identified (Section 4).
3. We empirically demonstrate that weighted retraining significantly benefits LSO across a variety of application domains and generative models, achieving substantial improvements over state-of-the-art methods on a widely-used chemical design benchmark (Section 6).

## 2 Problem Statement and Background

**Sample-Efficient Black Box Optimization** Let  $\mathcal{X}$  be an *input space*, and let  $f : \mathcal{X} \mapsto \mathbb{R}$  be an *objective function*. In particular, we focus on cases where 1) the input space  $\mathcal{X}$  is *high-dimensional* (i.e. 100+ effective dimensions) and *structured* (e.g. graphs, sequences or sets), and 2) the objective function  $f(\mathbf{x})$  is *black box* (i.e. no known analytic form or derivative information available) and is *expensive* to evaluate (e.g. in terms of time or energy cost). The *sample-efficient optimization* problem seeks to optimize  $f$  over  $\mathcal{X}$ , evaluating  $f$  as few times as possible, producing in the process a sequence of evaluated points  $\mathcal{D}_M \equiv \{\mathbf{x}_i, f(\mathbf{x}_i)\}_{i=1}^M$  with  $M$  function evaluations. Because there is no unambiguous metric to quantify sample-efficiency, it is generally good practice to plot any chosen metrics as a function of  $M$  to compare across multiple  $M$  values, and to report the expected value of any metric if an algorithm is stochastic; this is common practice in Bayesian optimization [50]. For a

fair comparison of different algorithms, in this work we choose to plot the expected  $K$ th best novel evaluated point as a function of  $M$ , for several values of  $K$ . We denote this as the Top $K$  score.

**Latent Space Optimization** LSO is a method for solving optimization problems, which defines a *latent space*  $\mathcal{Z}$ , a *generative model*  $g : \mathcal{Z} \mapsto \mathcal{X}$  that maps from latent space  $\mathcal{Z}$  to input space  $\mathcal{X}$ , and an *objective model*  $h : \mathcal{Z} \mapsto \mathbb{R}$  such that  $f(g(\mathbf{z})) \approx h(\mathbf{z}) \forall \mathbf{z} \in \mathcal{Z}$ . LSO is especially useful when  $\mathcal{X}$  is high-dimensional and/or structured, because  $\mathcal{Z}$  can be chosen to be a low-dimensional continuous space such as  $\mathbb{R}^n$ , *effectively turning a discrete optimization problem into a continuous one*, thereby allowing a wide array of well-studied and readily available optimization techniques to be applied. To realize this,  $g$  can be chosen to be a state-of-the-art deep generative model (DGM), such as a variational autoencoder (VAE) [28, 46] or a generative adversarial network (GAN) [14], which have been shown to be capable of learning vector representations of many types of high-dimensional, structured data [52, 2, 59, 7]. Furthermore,  $h$  can be chosen to be a probabilistic model such as a Gaussian process [62], which allows sample-efficient Bayesian optimization to be performed [3, 50]. To train  $h$ , one must find a corresponding latent point  $\mathbf{z}_i$  for each data point  $\mathbf{x}_i$  such that  $g(\mathbf{z}_i) \approx \mathbf{x}_i$ , which can be done by optimization in  $\mathcal{Z}$  or via an (approximate) inverse function  $q : \mathcal{X} \mapsto \mathcal{Z}$ .

### 3 Failure Modes of Latent Space Optimization

To understand the shortcomings of LSO, it is necessary to first examine in detail the role of the generative model, which is usually a DGM. State of the art DGMs such as VAEs and GANs are trained with a prior  $p(\mathbf{z})$  over the latent space  $\mathcal{Z}$ . This means that although the resulting function  $g : \mathcal{Z} \mapsto \mathcal{X}$  is defined over the entire latent space  $\mathcal{Z}$ , it is effectively only trained on points in regions of  $\mathcal{Z}$  with high probability under  $p$ . Importantly, even if  $\mathcal{Z}$  is an unbounded space with infinite volume such as  $\mathbb{R}^n$ , because  $p$  has finite volume, there must exist a *finite* subset  $\mathcal{Z}' \subset \mathcal{Z}$  that contains virtually all the probability mass of  $p$ .<sup>2</sup> We call  $\mathcal{Z}'$  the *feasible region* of  $\mathcal{Z}$ . Although in principle optimization can be performed over all of  $\mathcal{Z}'$ , it has been widely observed that optimizing outside of the feasible region tends to give poor results, yielding samples that are low-quality, or even invalid (e.g. invalid molecular strings, non-grammatical sentences); therefore all LSO methods known to us employ some sort of measure to restrict the optimization to near or within the feasible region [13, 29, 41, 15, 61, 35]. This means that LSO should be treated as a *bounded* optimization problem, whose feasible region is determined by  $p$ .

Informally, the training objective of  $g$  encourages points sampled from within the feasible region to match the data distribution that  $g$  was trained on, effectively “filling” the feasible region with points from the dataset,<sup>3</sup> such that a point’s relative volume roughly determined by its frequency in the training data. For many optimization problems, most of the the training data for the DGM is low-scoring (i.e. highly sub-optimal objective function values), thereby causing most of the feasible region to contain low-scoring points. Not only does this make the optimization problem more difficult to solve (like finding the proverbial “needle in a haystack”), but actually leaves insufficient space in the feasible region for a large number of novel, high-scoring points that lie outside the training distribution to be modelled by the DGM. Therefore, even a perfect optimization algorithm with unlimited evaluations of the objective function might be unable to find a novel point that is substantially better than the best point in the original dataset, simply because such a point may not exist in the feasible region.

This pathological behaviour is conceptually illustrated in Fig. 1a, where LSO is unable to find the global optimum that lies far from the training data, instead using its evaluation budget to find new points that lie within the feasible region, and close to the best points in the training set. We propose that this behaviour stems from two concrete problems in the LSO setup. The first problem is that the generative model’s training objective (to learn a latent space that captures the data distribution as closely as possible), does not necessarily match the true objective (to learn a latent space that is amenable to efficient optimization of the objective function). Put in terms of Fig. 1a, the feasible region that is learned, which uniformly and evenly surrounds the data points, is not the feasible region that would be useful for optimization, which would model more of the green region at the expense of the red region. The second problem is that information on new points acquired during the

<sup>2</sup> For example, a  $d$  dimensional Gaussian distribution has non-zero probability density everywhere, but almost all the probability mass in in a spherical shell of radius  $\sqrt{d}$ . See *this blog post* for a visualization.

<sup>3</sup>In VAEs, this is done explicitly through the use of an encoder.

iterative optimization procedure is not propagated to the generative model, where it could potentially help to refine and expand the coverage of the feasible region, uncovering new promising regions that an optimization algorithm can exploit. In terms of Fig. 1a, the new data is not used to shift the feasible region toward the green region, despite the optimization process indicating that this is a very promising region of  $\mathcal{X}$  for optimization. Luckily, we believe that neither of these two problems is inherent to LSO, and now pose a framework that directly addresses them.

## 4 Latent Space Optimization with Weighted Retraining

### 4.1 Training a Generative Model with a Weighted Training Objective

While it is unclear in general how to design a generative model that is maximally amenable to LSO, the argument presented in Section 3 suggests that it would at least be beneficial to dedicate a higher fraction of the feasible region to modelling high-scoring points. One obvious but inadequate method of achieving this is to simply discard all low-scoring points, e.g. by keeping only the top 10% of the data set, and use this reduced dataset to train the DGM. While this strategy could be feasible if data is plentiful, when data is scarce this option may not be viable because state of the art neural networks need a large amount of training data to avoid overfitting. This issue can be resolved by not viewing inclusion in the dataset as a binary choice, but instead as a *continuum* that can be realized by weighting the data points unevenly. If the generative model is trained on a distribution that systematically assigns more probability mass on high-scoring points and less mass on slow scoring points, the distribution-matching term in the DGM’s training objective will incentivize a larger fraction of the feasible region’s volume to be used to model high-scoring points, while simultaneously using all known data points to learn useful representations and avoid overfitting.

A simple way to achieve this weighting is to assign an explicit weight  $w_i$  to each data point, such that  $\sum_i w_i = 1$ . Recall training objective of common DGMs involves the expected value of a loss function  $\mathcal{L}$  with respect to the data distribution,<sup>4</sup> which is typically estimated using the empirical distribution over the training data  $\hat{p}(\mathbf{x}) = \frac{1}{N} \sum_{\mathbf{x}_i \in \mathcal{D}} \delta(\mathbf{x} - \mathbf{x}_i)$ : i.e.  $\mathbb{E}_{p(\mathbf{x})}[\mathcal{L}(\mathbf{x})] \approx \mathbb{E}_{\hat{p}(\mathbf{x})}[\mathcal{L}(\mathbf{x})] = \frac{1}{N} \sum_{\mathbf{x}_i \in \mathcal{D}} \mathcal{L}(\mathbf{x}_i)$ . If one uses  $w_i$  to construct a *weighted empirical distribution*  $\hat{p}_w(\mathbf{x}) = \sum_{\mathbf{x}_i \in \mathcal{D}} w_i \delta(\mathbf{x} - \mathbf{x}_i)$ , then one can apply importance weighting to use samples distributed according to  $\hat{p}_w(\mathbf{x})$  to estimate quantities with respect to  $\hat{p}_w(\mathbf{x})$ :

$$\mathbb{E}_{\hat{p}_w(\mathbf{x})}[\mathcal{L}(\mathbf{x})] = \mathbb{E}_{\hat{p}(\mathbf{x})} \left[ \frac{\hat{p}_w(\mathbf{x})}{\hat{p}(\mathbf{x})} \mathcal{L}(\mathbf{x}) \right] = \frac{1}{N} \sum_{\mathbf{x}_i \in \mathcal{D}} N w_i \mathcal{L}(\mathbf{x}_i) = \sum_{\mathbf{x}_i \in \mathcal{D}} w_i \mathcal{L}(\mathbf{x}_i) \quad (1)$$

In practice, Eq. (1) is difficult to minimize directly if the number of data points is large, motivating the use of stochastic gradient descent with mini-batches of size  $n \ll N$ :

$$\sum_{\mathbf{x}_i \in \mathcal{D}} w_i \mathcal{L}(\mathbf{x}_i) \approx \frac{N}{n} \sum_{j=1}^n w_j \mathcal{L}(\mathbf{x}_j) \quad (2)$$

If done naively, these mini-batches may have extremely high variance, especially if the variance of the weights is large. In practice, we found it was sufficient to reduce the variance of the weights by simply adding multiple copies of any  $\mathbf{x}_i$  with  $w_i > w_{\max}$ , then reducing the weight of each copy such that the sum is still  $w_i$ . More details on this are given in Appendix A.2.

We offer no universal rules for setting weights, except that all weights  $w_i$  should be restricted to strictly positive values, because a negative weight would incentivize the model to perform poorly, and a weight of zero is equivalent to discarding a point. This aside, there are many reasonable ways to choose the weights such that high-scoring points are weighted more, and low-scoring points are weighted less. In this work, we have decided to use a rank-based weight function,

$$w(\mathbf{x}; \mathcal{D}, k) \propto \frac{1}{kN + \text{rank}_{f, \mathcal{D}}(\mathbf{x})}, \quad \text{rank}_{f, \mathcal{D}}(\mathbf{x}) = |\{\mathbf{x}_i : f(\mathbf{x}_i) > f(\mathbf{x}), \mathbf{x}_i \in \mathcal{D}\}|, \quad (3)$$

which assigns a weight roughly proportional to the reciprocal (zero-based) rank of each data point. We chose Eq. (3) because it yields weights which are always positive, resilient to outliers, and has stable

<sup>4</sup> For a VAE,  $\mathcal{L}$  is the per-datapoint ELBO [28], while for a GAN,  $\mathcal{L}$  is the discriminator score [14]

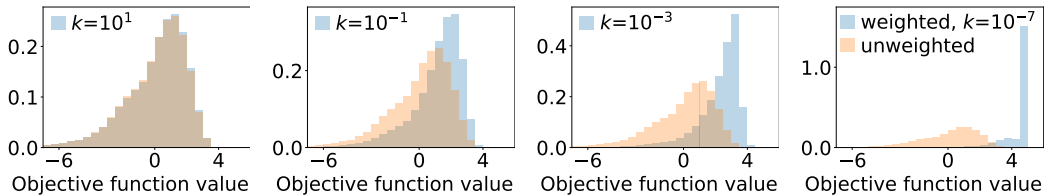


Figure 2: Distribution of objective function values of the ZINC dataset (see Section 6.3), weighted uniformly (orange) and with the rank weighting in Eq. (3) (blue). Large  $k$  approaches uniform weighting, while small  $k$  place most weight on the best (i.e., largest) objective function values.

behaviour over a range of dataset sizes (this is explained further in Appendix A.1). Furthermore, as shown in Fig. 2, it admits a single tunable hyperparameter  $k$  which controls the degree of weighting, where  $k = \infty$  corresponds to uniform weighting, i.e.  $w_i = \frac{1}{N}, \forall i$ , while  $k = 0$  places *all* mass on only the single point with the highest objective function value.

## 4.2 Periodic Retraining to Update the Latent Space

To allow the latent manifold to adapt to new information, we propose a conceptually simple solution: *periodically retraining the generative model* during the optimization procedure. In practice, this could be done by training a new model from scratch, or by fine-tuning the previously trained model on the novel data. However, as is often pointed out in the active learning literature, the effect of adding a few additional points to a large dataset is rather negligible, and thus it is unlikely that the generative model will change significantly if retrained on this augmented dataset [49]. While one could also retrain on *only* the new data, this might lead to the well-known phenomenon of catastrophic forgetting [37].

A key observation we make is that the *data weighting outlined in Section 4.1 actually resolves this problem*. Specifically, if the new points queried are high-scoring, then a suitable weighting scheme (such as Eq. (3)) will assign a large weight to them, while simultaneously decreasing the weights of many of the original data points, meaning that a small number of new points can have a disproportionate impact on the training distribution. If the generative model is then retrained using this distribution, it can be expected to change significantly to incorporate these new points prominently into the feasible region of the latent space. By contrast, if the new points queried are low-scoring, then the distribution will change negligibly, and the generative model will not significantly update, thereby avoiding adding new low-scoring points into the feasible region.

## 4.3 Weighted Retraining Combined

When put together, *data weighting* and *periodic retraining* complement each other elegantly, transforming the generative model from a passive decoding function into an active participant in the optimization process, whose role is to ensure that the latent manifold is constantly occupied by the most updated and relevant points for optimization. Their combined effect is visualized conceptually in Fig. 1b. Compared to Fig. 1a, in the first iteration in Fig. 1b the high-scoring pink point is given a higher weight, causing the feasible region to extend farther into the green region at the expense of the red region. This allows a better first point (orange) to be chosen relative to Fig. 1a. In the second iteration in Fig. 1b, weighted retraining on the orange point reshapes the latent space again, bringing the global optimum into the feasible region, where it is ultimately reached.

In the remainder of this text, we refer to the combination of these techniques as *weighted retraining* for brevity; see Algorithm 1 for pseudocode. We highlight that this algorithm is straightforward to implement in most models, with brief examples given in Appendix A.3. Computationally, the overhead of the weighting is minimal, and the cost of the retraining can be reduced by fine-tuning an existing model on the weighted distribution instead of retraining it from scratch. Although this may still be prohibitively expensive for some applications, we stress that in many scenarios the cost of training a model is insignificant compared to even a single evaluation of the objective function (e.g. performing wet-lab experiments for drug design), making weighted retraining a sensible choice.

---

**Algorithm 1** Latent Space Optimization with Weighted Retraining (changes highlighted in blue)

---

```
1: Input: Data  $\mathcal{D} = \{(\mathbf{x}_i, f(\mathbf{x}_i))\}_{i=1}^N$ , evaluation budget  $M$ , objective function  $f(\mathbf{x})$ , generative model  $g(\mathbf{z})$ , inverse model  $q(\mathbf{x})$ , retrain budget  $R$ , weighting function  $w(\mathbf{x})$ 
2: for  $1, \dots, R$  do
3:   Train generative model  $g$  and inverse model  $q$  on data  $\mathcal{D}$  weighted by  $\mathcal{W} = \{w(\mathbf{x})\}_{\mathbf{x} \in \mathcal{D}}$ 
4:   for  $1, \dots, M/R$  do
5:     Compute latent variables  $\mathcal{Z} = \{\mathbf{z} = q(\mathbf{x})\}_{\mathbf{x} \in \mathcal{D}}$ 
6:     Fit objective model  $h$  to  $\mathcal{Z}$  and  $\mathcal{D}$ , and suggest new latent  $\tilde{\mathbf{z}}$  based on  $h$ 
7:     Obtain corresponding input  $\tilde{\mathbf{x}} = g(\tilde{\mathbf{z}})$ , evaluate  $f(\tilde{\mathbf{x}})$  and set  $\mathcal{D} \leftarrow \mathcal{D} \cup \{(\tilde{\mathbf{x}}, f(\tilde{\mathbf{x}}))\}$ 
8:   end for
9: end for
10: Output: Augmented dataset  $\mathcal{D}$ 
```

---

## 5 Related Work

While a large body of work is applicable to the general problem formulated in Section 2 (both using and not using machine learning), in this section we focus only on the most relevant machine learning literature. Early formulations of LSO were motivated by scaling Gaussian processes to high dimensional problems with simple linear manifolds, using either random projections [60] or a learned transformation matrix [12]. LSO using DGMs was first applied to chemical design in [13], and further built upon in subsequent papers [21, 29, 9, 24, 5, 15, 35]. It has also been applied to other field such as automatic machine learning [33, 34], and conditional image generation [41, 40]. If the optimization model is a Gaussian process, the DGM can be viewed as a form of “extended kernel”, making LSO conceptually related to deep kernel learning [63, 19].

There are several previous papers that have used ideas closely related to weighted retraining. Perhaps the closest model to ours is the Feedback GAN [17], wherein samples are generated with a GAN and evaluated, discarding samples with low scores. These  $n$  samples replace the  $n$  oldest points in the training set, after which the GAN is retrained on the new dataset. This can be viewed as a crude version of weighted retraining, only using the weights 0 and  $1/N$ , and assigning weights not based on scores but on novelty. Similarly, in [48] a generative model is trained on drug-like molecules, then repeatedly sampled, evaluating all samples and keeping only those with high scores. The model is then fine-tuned on the high-scoring samples and this process is repeated. Again, this can be viewed as a special case of weighted retraining, where the weights are implicitly defined by the number of fine-tuning epochs. Furthermore, both of these techniques are purely generative and have no optimization component, so we believe that they are fundamentally sample inefficient.

*Bayesian optimization (BO)* is a technique that maintains a probabilistic model of the objective function, and chooses new points to evaluate based on the modelled distribution of the objective value at unobserved points. BO is widely viewed as the go-to framework for sample-efficient black-box optimization [3, 53]. However, most practical BO models exist for continuous, low-dimensional spaces [50]. While recent works have tried to develop models to extend BO to either structured [1, 27, 6, 42] or high-dimensional [25, 39, 18] input spaces, we are not aware of any BO method that can efficiently handle the types of high-dimensional and structured spaces considered in this work.

*Reinforcement learning (RL)* frames optimization problems as Markov decision processes for which an agent learns an optimal policy [55]. It has recently been applied to various optimization problems in structured input spaces [30], notably in chemical design [64, 65, 16, 43, 45, 51]. While RL is undoubtedly effective at optimization, it is generally extremely sample inefficient, and consequently its biggest successes are in virtual environments where function evaluations are inexpensive [30].

Finally, one interesting direction is the development of *conditional generative models*, which directly produce novel points conditioned on a specific property value [54, 38]. Although many variants of these algorithms have been applied to real-world problems such as chemical design [22, 26, 31, 32, 4], the sample efficiency of this paradigm is currently unclear.

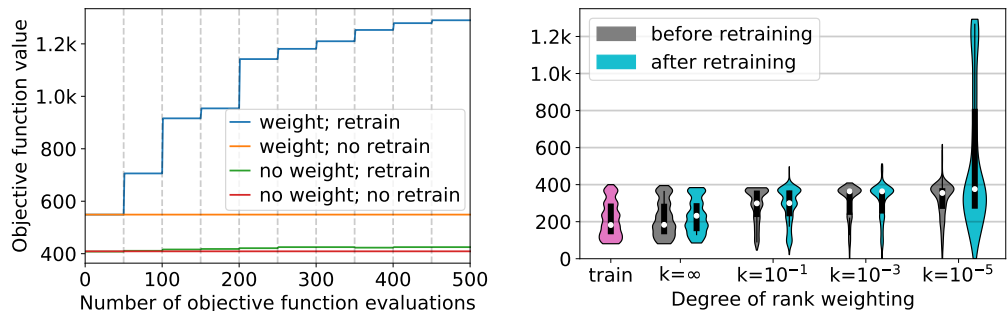


Figure 3: (Left) Top1 scores of the shapes found by the different methods, showing that weighted retraining performs best by a substantial margin. (Right) Distributions of areas of shapes from the training set, and of shapes sampled from the generative model’s prior, for  $k \in [\infty, 10^{-1}, 10^{-3}, 10^{-5}]$ .

## 6 Empirical Evaluation

We demonstrate the effectiveness of weighted retraining on a toy task involving binary shapes, on an arithmetic expression fitting task, and on a real-world chemical-design task, and show that it substantially improves the sample-efficiency of state-of-the-art algorithms. On each task, we compare the following four settings: 1) Neither retraining nor weighting (i.e., the default for current methods), 2) retraining but no weighting, 3) weighting but no retraining (i.e., using a fixed model that was initially trained on a weighted dataset), and 4) both weighting and retraining. Following Section 2, we report results by plotting the expected TopK score as a function of the number of objective function evaluations, in contrast to previous works which typically report only final scores, and take the maximum across seeds rather than the average [13, 29, 5, 21]. We furthermore use the shape task to validate some of the conjectures made in Sections 3 and 4.

### 6.1 2D Shape Area Maximization Task

We train a convolutional VAE on the dSprites dataset [36], which consists of images of size  $64 \times 64$  containing 2D shapes with different scales, rotations, and positions. We use the 245,760 square shapes in the dataset for simplicity. The images are binary, i.e.  $\mathbf{x} \in \{0, 1\}^{64 \times 64}$ , where pixels with values  $x_i = 0$  and  $x_i = 1$  belong to the background and the shape, respectively. Our goal is to generate a shape  $\mathbf{x}$  with *maximum area*, where area is defined as the sum of all pixel values, i.e.  $\arg \max_{\mathbf{x}} \sum_{i=1}^{64 \times 64} x_i$ , which is achieved if and only if all pixels are set to 1, i.e.  $\mathbf{x}^* = [1]_{i=1}^{64 \times 64}$ .

First, we train models using rank weighting with different  $k$  values, to validate that weighted training changes the learned space to include more high-performing points. We measure this change by sampling shapes from the prior of each model. Fig. 3 (right) confirms that lower  $k$  values do lead to a significant change in the contents of the latent space. Next, we perform weighted retraining with 500 objective evaluations, retraining after every 50th, using  $k = 10^{-5}$  for the weighting. To illustrate what a strong optimization algorithm could achieve, we do a form of exhaustive search which evaluates all latent points on the grid  $[-5.0, -4.5, \dots, 4.5, 5.0]^5$  that have an  $\ell_2$ -norm of at most 5, and choose the 50 (500) shapes with the largest area for the variants with retraining (without retraining). Fig. 3 (left) shows that weighted retraining substantially outperforms all other baselines. Note that there are no error bars in Fig. 3 as the optimization procedure we use is deterministic.

### 6.2 Arithmetic Expression Fitting Task

We consider the task of generating an arithmetic expression  $\mathbf{x}$  that best fits a target expression  $\mathbf{x}^*$ , given a training set of 50,000 univariate arithmetic expressions generated from a formal grammar [29]. Examples of such expressions are  $\sin(2)$ ,  $v/(3+1)$  and  $v/2 * \exp(v)/\sin(2*v)$ , which are all considered to be functions of some variable  $v$ . Following [29], the objective is to find an expression with minimal mean squared error to the target expression  $\mathbf{x}^* = 1/3 * v * \sin(v*v)$ , computed over 1000 evenly-spaced points between  $-10$  and  $+10$ . We use rank weighting with  $k = 10^{-3}$ , a grammar VAE as the generative model [29], and a sparse Gaussian process (SGP) [56]



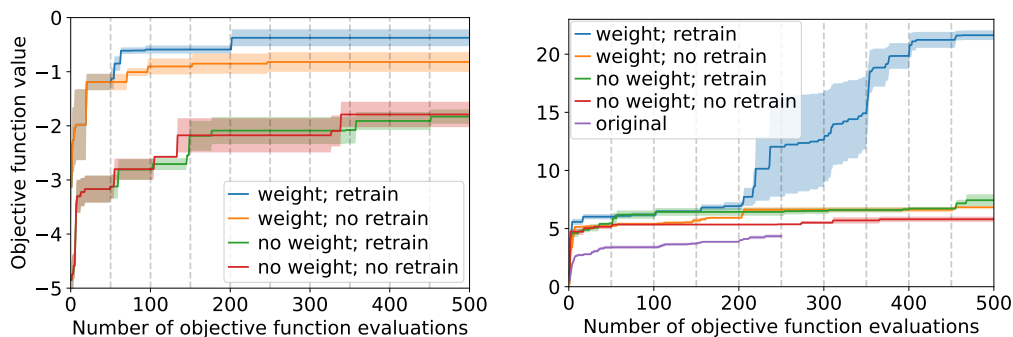


Figure 4: Mean  $\pm$  one standard error (over 3 random seeds) of the Top1 scores on the arithmetic expression fitting task (left) and the chemical design task (right), using rank weighting with  $k = 10^{-3}$ . (Right) The purple line labelled “original” shows the results from [21], extracted from their GitHub repository. Weighted retraining achieves significantly better optimization performance and higher sample efficiency than the baselines on both tasks, and in particular on the chemical design task.

as the optimization model. More details are given in Appendix C. The results are shown in Fig. 4 (left), roughly matching those in Fig. 3 (left), wherein weighting and retraining individually improve performance, and the combination of weighting and retraining achieves the best performance.

### 6.3 Real-World Chemical Design Task

We follow [13] and optimize the drug properties of molecules. In particular, we consider the standardized task originally proposed in [29] of synthesizing a molecule with maximal penalized *water-octanol partition coefficient* ( $\log P$ ), starting from the molecules in the ZINC250k molecule dataset [20] (see Appendix C.6 for more details). In choosing this task, we follow a series of papers which perform optimization in chemical space [29, 5, 21, 65, 64], allowing the effect of weighted retraining to be quantitatively compared to other approaches. These works have demonstrated that the choice of DGM has a substantial effect on both validity of samples from the latent space, and the resulting optimization performance in this space; therefore, to isolate the effect of weighted retraining, we use the junction tree VAE [21], which to our knowledge is the state-of-the-art model on this task.

To be directly comparable to previous results, we use the pre-trained model provided in the GitHub repository of [21] as the unweighted model, and create weighted models by fine-tuning the pre-trained model for 1 epoch over the entire weighted dataset. We retrain after every 50th function evaluation, doing only fine tuning for computational efficiency. The results are shown in Fig. 4 (right), using  $k = 10^{-3}$ . Similar to the arithmetic expression task, both weighting and retraining helps individually, with weighted retraining together significantly outperforming all other methods. Similar to Fig. 3 (left), the performance can be seen to significantly improve immediately after several of the retraining steps, suggesting that the retraining does indeed incorporate new information into the latent space, as conjectured. Compared to previous works, the scores achieved in this paper not only beat the results of all previous methods, but do so using far fewer samples. The best previously known score was 11.84 and was obtained with  $\approx 5000$  samples [65]. By contrast, our best score is 22.55, and was achieved with only 500 samples (see Table 1 for a more detailed comparison). Additional plots and more information can be found in Appendices B and C.

## 7 Conclusion

We proposed a method for efficient black-box optimization over high-dimensional, structured input spaces, combining latent space optimization with weighted retraining. We showed that while being conceptually simple and easy to implement on top of previous methods, weighted retraining significantly boosts their efficiency and performance on challenging real-world optimization problems.

There are many avenues for future work. Firstly, we observed that weighted retraining was less beneficial when used with poorly-performing optimization algorithms. The latent space of DGMs



can be challenging to optimize over, motivating further research to optimize more effectively and/or make the space more amenable to optimization. Another promising idea is the use of a weighting *schedule* instead of a fixed weighting, which may allow balancing exploration vs. exploitation similar to simulated annealing [58]. A further interesting direction would be to consider different classes of weighting functions, particularly those that are robust to noise in the objective function evaluations. Finally, we are eager to apply our approach to more real-world problems. We envision weighted retraining to become a core component of model-based optimization methods, further establishing machine learning as a critical tool for advancing science and engineering.

## Broader Impact

Ultimately, this work is preliminary, despite the promise of latent space optimization, there may still be significant obstacles to applying it more widely in the real world. That aside, we believe that the primary effect of this line of research will be to enable faster discoveries of novel entities, such as new medicines, new energy materials, or new device designs. The worldwide effort to develop vaccines and treatments for the COVID-19 pandemic has highlighted the importance of techniques for fast, targeted discovery using only small amounts of data: we have seen that even if the whole world is devoted to performing experiments with a single goal, the sheer size of the search space means that sample efficiency is still important.

As much as this technology could be used to discover good things, it could also be used to discover bad things (e.g. chemical/biological weapons). However, as substantial resources and infrastructure are required to produce these, we do not expect that this line of work will enable new parties to begin their development. Rather, at worse, it may allow people who are already involved in their development to do it slightly more effectively.

Finally, we believe that this line of work has the potential to influence other problem areas in machine learning, such as conditional image generation and conditional text generation, because these tasks can also be viewed as optimization, whose objective function is a human judgement, which is generally expensive to obtain.

## Acknowledgments and Disclosure of Funding

We thank Ross Clarke, Gregor Simm, David Burt, and Javier Antorán for insightful feedback and discussions. AT acknowledges funding via a C T Taylor Cambridge International Scholarship. ED acknowledges funding by the EPSRC and Qualcomm. This work has been performed using resources provided by the Cambridge Tier-2 system operated by the University of Cambridge Research Computing Service (<http://www.hpc.cam.ac.uk>) funded by EPSRC Tier-2 capital grant EP/P020259/1.

## References

- [1] R. Baptista and M. Poloczek. Bayesian optimization of combinatorial structures. *arXiv preprint arXiv:1806.08838*, 2018.
- [2] S. R. Bowman, L. Vilnis, O. Vinyals, A. M. Dai, R. Jozefowicz, and S. Bengio. Generating Sentences from a Continuous Space. *arXiv:1511.06349 [cs]*, May 2016. arXiv: 1511.06349.
- [3] E. Brochu, V. M. Cora, and N. De Freitas. A tutorial on bayesian optimization of expensive cost functions, with application to active user modeling and hierarchical reinforcement learning. *arXiv preprint arXiv:1012.2599*, 2010.
- [4] D. H. Brookes and J. Listgarten. Design by adaptive sampling. *arXiv:1810.03714 [cs, q-bio, stat]*, Feb 2020. arXiv: 1810.03714.
- [5] H. Dai, Y. Tian, B. Dai, S. Skiena, and L. Song. Syntax-Directed Variational Autoencoder for Structured Data. *arXiv:1802.08786 [cs]*, Feb. 2018. arXiv: 1802.08786.
- [6] E. Daxberger, A. Makarova, M. Turchetta, and A. Krause. Mixed-variable bayesian optimization. *arXiv preprint arXiv:1907.01329*, 2019.
- [7] N. Cao and T. Kipf. MolGAN: An implicit generative model for small molecular graphs. *arXiv:1805.11973 [cs, stat]*, May 2018. arXiv: 1805.11973.

- [8] A. G. De G. Matthews, M. Van Der Wilk, T. Nickson, K. Fujii, A. Boukouvalas, P. León-Villagrà, Z. Ghahramani, and J. Hensman. Gpflow: A gaussian process library using tensorflow. *The Journal of Machine Learning Research*, 18(1):1299–1304, 2017.
- [9] S. Eismann, D. Levy, R. Shu, S. Bartsch, and S. Ermon. Bayesian optimization and attribute adjustment. In *Proceedings of the Thirty-Fourth Conference (2018)*, page 11, Monterey, California, USA, Aug. 2018. Association for Uncertainty in Artificial Intelligence.
- [10] T. Elsken, J. H. Metzen, and F. Hutter. Neural Architecture Search: A Survey. *Journal of Machine Learning Research*, 20(55):1–21, 2019.
- [11] D. Elton, Z. Boukouvalas, M. Fuge, and P. Chung. Deep learning for molecular design—a review of the state of the art. *Molecular Systems Design & Engineering*, 4(4):828–849, 2019. Publisher: Royal Society of Chemistry.
- [12] R. Garnett, M. A. Osborne, and P. Hennig. Active Learning of Linear Embeddings for Gaussian Processes. *arXiv:1310.6740 [cs, stat]*, Oct. 2013. arXiv: 1310.6740.
- [13] R. Gómez-Bombarelli, J. N. Wei, D. Duvenaud, J. M. Hernández-Lobato, B. Sánchez-Lengeling, D. Sheberla, J. Aguilera-Iparraguirre, T. D. Hirzel, R. P. Adams, and A. Aspuru-Guzik. Automatic chemical design using a data-driven continuous representation of molecules. *ACS central science*, 4(2):268–276, 2018.
- [14] I. Goodfellow, J. Pouget-Abadie, M. Mirza, B. Xu, D. Warde-Farley, S. Ozair, A. Courville, and Y. Bengio. Generative adversarial nets. In *Advances in neural information processing systems*, pages 2672–2680, 2014.
- [15] R.-R. Griffiths and J. Miguel Hernández-Lobato. Constrained Bayesian optimization for automatic chemical design using variational autoencoders. *Chemical Science*, 11(2):577–586, 2020. Publisher: Royal Society of Chemistry.
- [16] G. L. Guimaraes, B. Sanchez-Lengeling, C. Outeiral, P. L. C. Farias, and A. Aspuru-Guzik. Objective-Reinforced Generative Adversarial Networks (ORGAN) for Sequence Generation Models. *arXiv:1705.10843 [cs, stat]*, Feb. 2018. arXiv: 1705.10843.
- [17] A. Gupta and J. Zou. Feedback GAN for DNA optimizes protein functions. *Nature Machine Intelligence*, 1(2):105–111, Feb. 2019. Number: 2 Publisher: Nature Publishing Group.
- [18] T. N. Hoang, Q. M. Hoang, R. Ouyang, and K. H. Low. Decentralized high-dimensional bayesian optimization with factor graphs. In *Thirty-Second AAAI Conference on Artificial Intelligence*, 2018.
- [19] W. Huang, D. Zhao, F. Sun, H. Liu, and E. Chang. Scalable Gaussian Process Regression Using Deep Neural Networks. In *Twenty-Fourth International Joint Conference on Artificial Intelligence*, June 2015.
- [20] J. J. Irwin, T. Sterling, M. M. Mysinger, E. S. Bolstad, and R. G. Coleman. ZINC: A Free Tool to Discover Chemistry for Biology. *Journal of Chemical Information and Modeling*, 52(7):1757–1768, July 2012. Publisher: American Chemical Society.
- [21] W. Jin, R. Barzilay, and T. Jaakkola. Junction Tree Variational Autoencoder for Molecular Graph Generation. *arXiv:1802.04364 [cs, stat]*, Mar. 2019. arXiv: 1802.04364.
- [22] W. Jin, K. Yang, R. Barzilay, and T. Jaakkola. Learning Multimodal Graph-to-Graph Translation for Molecular Optimization. *arXiv:1812.01070 [cs, stat]*, Jan. 2019. arXiv: 1812.01070.
- [23] D. R. Jones, M. Schonlau, and W. J. Welch. Efficient global optimization of expensive black-box functions. *Journal of Global optimization*, 13(4):455–492, 1998.
- [24] H. Kajino. Molecular Hypergraph Grammar with Its Application to Molecular Optimization. In *International Conference on Machine Learning*, pages 3183–3191, May 2019. ISSN: 1938-7228 Section: Machine Learning.
- [25] K. Kandasamy, J. Schneider, and B. Póczos. High dimensional bayesian optimisation and bandits via additive models. In *International Conference on Machine Learning*, pages 295–304, 2015.
- [26] S. Kang and K. Cho. Conditional Molecular Design with Deep Generative Models. *Journal of Chemical Information and Modeling*, 59(1):43–52, Jan. 2019.
- [27] J. Kim, M. McCourt, T. You, S. Kim, and S. Choi. Bayesian optimization over sets. *arXiv preprint arXiv:1905.09780*, 2019.

- [28] D. P. Kingma and M. Welling. Auto-encoding variational bayes. *arXiv preprint arXiv:1312.6114*, 2013.
- [29] M. J. Kusner, B. Paige, and J. M. Hernández-Lobato. Grammar variational autoencoder. In *Proceedings of the 34th International Conference on Machine Learning - Volume 70, ICML'17*, pages 1945–1954, Sydney, NSW, Australia, Aug. 2017. JMLR.org.
- [30] Y. Li. Deep Reinforcement Learning. *arXiv:1810.06339 [cs, stat]*, Oct. 2018. arXiv: 1810.06339.
- [31] Y. Li, L. Zhang, and Z. Liu. Multi-objective de novo drug design with conditional graph generative model. *Journal of Cheminformatics*, 10(1):33, July 2018.
- [32] J. Lim, S. Ryu, J. W. Kim, and W. Y. Kim. Molecular generative model based on conditional variational autoencoder for de novo molecular design. *Journal of Cheminformatics*, 10(1):31, July 2018.
- [33] X. Lu, J. Gonzalez, Z. Dai, and N. Lawrence. Structured variationally auto-encoded optimization. In *International Conference on Machine Learning*, pages 3267–3275, 2018.
- [34] R. Luo, F. Tian, T. Qin, E. Chen, and T.-Y. Liu. Neural architecture optimization. In *Advances in neural information processing systems*, pages 7816–7827, 2018.
- [35] O. Mahmood and J. M. Hernández-Lobato. A COLD Approach to Generating Optimal Samples. *arXiv:1905.09885 [cs, q-bio, stat]*, May 2019. arXiv: 1905.09885.
- [36] L. Matthey, I. Higgins, D. Hassabis, and A. Lerchner. dsprites: Disentanglement testing sprites dataset. <https://github.com/deepmind/dsprites-dataset/>, 2017.
- [37] M. McCloskey and N. J. Cohen. Catastrophic Interference in Connectionist Networks: The Sequential Learning Problem. In G. H. Bower, editor, *Psychology of Learning and Motivation*, volume 24, pages 109–165. Academic Press, Jan. 1989.
- [38] M. Mirza and S. Osindero. Conditional Generative Adversarial Nets. *arXiv:1411.1784 [cs, stat]*, Nov. 2014. arXiv: 1411.1784.
- [39] M. Mutny and A. Krause. Efficient high dimensional bayesian optimization with additivity and quadrature fourier features. In *Advances in Neural Information Processing Systems*, pages 9005–9016, 2018.
- [40] A. Nguyen, J. Clune, Y. Bengio, A. Dosovitskiy, and J. Yosinski. Plug & Play Generative Networks: Conditional Iterative Generation of Images in Latent Space. pages 4467–4477, 2017.
- [41] A. Nguyen, A. Dosovitskiy, J. Yosinski, T. Brox, and J. Clune. Synthesizing the preferred inputs for neurons in neural networks via deep generator networks. In D. D. Lee, M. Sugiyama, U. V. Luxburg, I. Guyon, and R. Garnett, editors, *Advances in Neural Information Processing Systems 29*, pages 3387–3395. Curran Associates, Inc., 2016.
- [42] C. Oh, J. M. Tomczak, E. Gavves, and M. Welling. Combinatorial bayesian optimization using graph representations. *arXiv preprint arXiv:1902.00448*, 2019.
- [43] M. Olivecrona, T. Blaschke, O. Engkvist, and H. Chen. Molecular de-novo design through deep reinforcement learning. *Journal of Cheminformatics*, 9(1):48, Sept. 2017.
- [44] D. W. Otter, J. R. Medina, and J. K. Kalita. A Survey of the Usages of Deep Learning for Natural Language Processing. *IEEE Transactions on Neural Networks and Learning Systems*, pages 1–21, 2020. Conference Name: IEEE Transactions on Neural Networks and Learning Systems.
- [45] M. Popova, O. Isayev, and A. Tropsha. Deep reinforcement learning for de novo drug design. *Science Advances*, 4(7):eaap7885, July 2018.
- [46] D. J. Rezende, S. Mohamed, and D. Wierstra. Stochastic backpropagation and approximate inference in deep generative models. *arXiv preprint arXiv:1401.4082*, 2014.
- [47] B. Sanchez-Lengeling and A. Aspuru-Guzik. Inverse molecular design using machine learning: Generative models for matter engineering. *Science*, 361(6400):360–365, July 2018.
- [48] M. H. S. Segler, T. Kogej, C. Tyrchan, and M. P. Waller. Generating Focused Molecule Libraries for Drug Discovery with Recurrent Neural Networks. *ACS Central Science*, 4(1):120–131, Jan. 2018. Publisher: American Chemical Society.

- [49] O. Sener and S. Savarese. Active Learning for Convolutional Neural Networks: A Core-Set Approach. *arXiv:1708.00489 [cs, stat]*, June 2018. arXiv: 1708.00489.
- [50] B. Shahriari, K. Swersky, Z. Wang, R. P. Adams, and N. De Freitas. Taking the human out of the loop: A review of bayesian optimization. *Proceedings of the IEEE*, 104(1):148–175, 2015.
- [51] G. N. C. Simm, R. Pinsler, and J. M. Hernández-Lobato. Reinforcement Learning for Molecular Design Guided by Quantum Mechanics. *arXiv:2002.07717 [cs, stat]*, Feb. 2020. arXiv: 2002.07717.
- [52] M. Simonovsky and N. Komodakis. GraphVAE: Towards Generation of Small Graphs Using Variational Autoencoders. Feb. 2018.
- [53] J. Snoek, H. Larochelle, and R. P. Adams. Practical bayesian optimization of machine learning algorithms. In *Advances in neural information processing systems*, pages 2951–2959, 2012.
- [54] K. Sohn, H. Lee, and X. Yan. Learning Structured Output Representation using Deep Conditional Generative Models. In C. Cortes, N. D. Lawrence, D. D. Lee, M. Sugiyama, and R. Garnett, editors, *Advances in Neural Information Processing Systems 28*, pages 3483–3491. Curran Associates, Inc., 2015.
- [55] R. S. Sutton, A. G. Barto, et al. *Introduction to reinforcement learning*, volume 135. MIT press Cambridge, 1998.
- [56] M. Titsias. Variational learning of inducing variables in sparse gaussian processes. In *Artificial Intelligence and Statistics*, pages 567–574, 2009.
- [57] A. van den Oord, N. Kalchbrenner, L. Espeholt, k. kavukcuoglu, O. Vinyals, and A. Graves. Conditional Image Generation with PixelCNN Decoders. In D. D. Lee, M. Sugiyama, U. V. Luxburg, I. Guyon, and R. Garnett, editors, *Advances in Neural Information Processing Systems 29*, pages 4790–4798. Curran Associates, Inc., 2016.
- [58] P. J. Van Laarhoven and E. H. Aarts. Simulated annealing. In *Simulated annealing: Theory and applications*, pages 7–15. Springer, 1987.
- [59] H. Wang, J. Wang, J. Wang, M. Zhao, W. Zhang, F. Zhang, X. Xie, and M. Guo. GraphGAN: Graph Representation Learning With Generative Adversarial Nets. In *Thirty-Second AAAI Conference on Artificial Intelligence*, Apr. 2018.
- [60] Z. Wang, M. Zoghi, F. Hutter, D. Matheson, and N. d. Freitas. Bayesian Optimization in High Dimensions via Random Embeddings. In *Twenty-Third International Joint Conference on Artificial Intelligence*, June 2013.
- [61] T. White. Sampling Generative Networks. *arXiv:1609.04468 [cs, stat]*, Dec. 2016. arXiv: 1609.04468.
- [62] C. K. Williams and C. E. Rasmussen. *Gaussian processes for machine learning*, volume 2. MIT press Cambridge, MA, 2006.
- [63] A. G. Wilson, Z. Hu, R. Salakhutdinov, and E. P. Xing. Deep Kernel Learning. In *Artificial Intelligence and Statistics*, pages 370–378, May 2016. ISSN: 1938-7228 Section: Machine Learning.
- [64] J. You, B. Liu, Z. Ying, V. Pande, and J. Leskovec. Graph Convolutional Policy Network for Goal-Directed Molecular Graph Generation. In S. Bengio, H. Wallach, H. Larochelle, K. Grauman, N. Cesa-Bianchi, and R. Garnett, editors, *Advances in Neural Information Processing Systems 31*, pages 6410–6421. Curran Associates, Inc., 2018.
- [65] Z. Zhou, S. Kearnes, L. Li, R. N. Zare, and P. Riley. Optimization of Molecules via Deep Reinforcement Learning. *Scientific Reports*, 9(1):1–10, July 2019. Number: 1 Publisher: Nature Publishing Group.

## A Details on the Weighting Function

### A.1 More Information on Rank-Based Weighting

**Independence from Dataset Size** We show that the key properties of rank-based weighting depend *only* on  $k$ , and not on the dataset size  $N$ , meaning that applying rank weighting with a fixed  $k$  to differently sized datasets will yield similar results. In particular, we show that under mild assumptions, the fraction of weights devoted to a particular quantile of the data depends on  $k$  but not  $N$ .

Suppose that the quantile of interest is the range  $q_1$ – $q_2$  (for example, the first quartile corresponds to the range 0–0.25). This corresponds approximately to the points with ranks  $q_1N$ – $q_2N$ . We make the following assumptions:

1.  $kN \gg 1$
2.  $kN$  is approximately integer valued, which is realistic if  $N \gg 1/k$
3.  $q_1$  and  $q_2$  are chosen so that  $q_1N$  and  $q_2N$  are integers.

Because the ranks form the sequence  $0, 1, \dots, N-1$ , under the above assumptions all weights are reciprocal integers, so the sum of the rank weights is strongly connected to the harmonic series. Recall that the partial sum of the harmonic series can be approximated by the natural logarithm:

$$\sum_{j=1}^N \frac{1}{j} \approx \ln N + \gamma \quad (4)$$

Here,  $\gamma$  is the Euler–Mascheroni constant. The fraction of the total weight devoted to the quantile  $q_1$ – $q_2$  can be found by summing the weights of points with rank  $q_1N$ – $q_2N$ , and dividing by the normalization constant (the sum of all weights). First, because  $kN \gg 1$  implies that  $(kN-1) \approx kN$ , the sum of all the weights can be expressed as:

$$\begin{aligned} \sum_{r=0}^{N-1} w(\mathbf{x}_r; \mathcal{D}, k) &= \sum_{r=0}^{N-1} \frac{1}{kN+r} \\ &= \sum_{r=1}^{kN+(N-1)} \frac{1}{r} - \sum_{r'=1}^{kN-1} \frac{1}{r'} \\ &\approx (\ln((k+1)N-1) + \gamma) - (\ln(kN-1) + \gamma) \\ &= \ln \frac{(k+1)N-1}{kN-1} \approx \ln \frac{(k+1)N}{kN} = \ln \left(1 + \frac{1}{k}\right) \end{aligned}$$

Note that this does not depend on the dataset size  $N$ . Second, using the same assumption, the sum of the weights in the quantile is:

$$\begin{aligned} \sum_{r=q_1N}^{q_2N} w(\mathbf{x}_r; \mathcal{D}, k) &= \sum_{r=q_1N}^{q_2N} \frac{1}{kN+r} \\ &= \sum_{r=1}^{(k+q_2)N} \frac{1}{r} - \sum_{r'=1}^{(k+q_1)N-1} \frac{1}{r'} \\ &\approx (\ln((k+q_2)N-1) + \gamma) - (\ln((k+q_1)N-1) + \gamma) \\ &= \ln \frac{(k+q_2)N}{(k+q_1)N-1} \approx \ln \frac{(k+q_2)N}{(k+q_1)N} = \ln \frac{(k+q_2)}{(k+q_1)} \end{aligned}$$

which is also independent of  $N$ . Therefore, the fraction of the total weight allocated to a given quantile of data is *independent of  $N$* , being only dependent on  $k$ . Although the analysis that led to this result made some assumptions about certain values being integers, in practice the actual distributions of weights are extremely close to what this analysis predicts. Fig. 5 shows the allocation of the

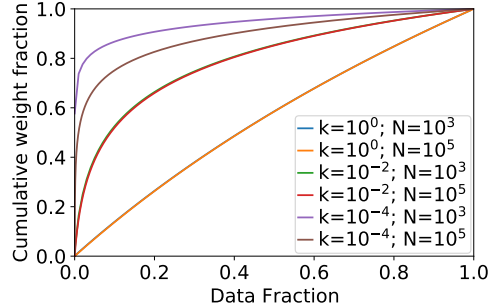


Figure 5: Cumulative distribution of rank weights (sorted highest to lowest), showing a distribution that is independent of  $N$  if  $kN > 1$ .

weights to different quantiles of the datasets. For  $kN > 1$ , the distribution is essentially completely independent of  $N$ . Only when  $kN < 1$  this fails to hold.

Finally, we discuss some potential questions about the rank-based weighting.

**Why do the weights need to be normalized?** If the objective is to minimize  $\sum_{\mathbf{x}_i \in \mathcal{D}} w_i \mathcal{L}(\mathbf{x}_i)$ , for any  $a > 0$ , minimizing  $a \sum_{\mathbf{x}_i \in \mathcal{D}} w_i \mathcal{L}(\mathbf{x}_i)$  is an equivalent problem. Therefore, in principle, the absolute scale of the weights does not matter, and so the weights do not *need* to be normalized, even if this precludes their interpretation as a probability distribution. However, in practice, if minimization is performed using gradient-based algorithms, then the scaling factor for the weights is also applied to the gradients, possibly requiring different hyperparameter settings (such as a different learning rate). By normalizing the weights, it is easier to identify hyperparameter settings that work robustly across different problems, thereby allowing weighted retraining to be applied with minimal tuning.

**Why not use a weight function directly based on the objective function value?** Although there is nothing inherently flawed about using such a weight function, there are some practical difficulties.

- Such a weight function would either be bounded (in which case values beyond a certain threshold would all be weighted equally), or it would be very sensitive to outliers (i.e. extremely high or low values which would directly cause the weight function to take on an extremely high or low value). This is extremely important because the weights are *normalized*, so one outlier would also affect the values of all other points.
- Such a weight function would not be invariant to simple transformations of the objective function. For example, if the objective function is  $f$ , then maximizing  $f(\mathbf{x})$  or  $f_{ab}(\mathbf{x}) = af(\mathbf{x}) + b$  is an equivalent problem (for  $a > 0$ ), but would yield different weights. This would effectively introduce scale hyperparameters into the weight function, which is undesirable.

## A.2 Mini-Batching with Variance Reduction for Weighted Training

The following is a Python code snippet of an implementation of the variance reduction:

```
def reduce_variance(data, weights, w_max):
    new_data = []
    new_weights = []
    for x, w in zip(data, weights):
        if w <= w_max: # If it is less than the max weight, just add it
            new_data.append(x)
            new_weights.append(w)
        else: # Otherwise, add multiple copies
            n_copies = int(math.ceil(w / w_max))
            new_data += [x] * n_copies
            new_weights += [w / n_copies] * n_copies
    return new_data, new_weights
```

The parameter `w_max` was typically set to 5.0, which was chosen to both reduce the variance, while simultaneously not increasing the dataset size too much. Note that this was applied *after* the weights were normalized.

Another way to reduce the variance would be to sample the minibatches using the weighted distribution and not directly apply the weights when calculating the loss, since they would be applied implicitly through the sampling. While this is conceptually simpler, and in some cases easier to implement, it may necessitate many passes through the dataset to sample every data point if the weights are highly non-uniform. We chose to avoid this, although we conjecture that this should also be a valid way to implement weighted retraining with reduced variance.

Regardless of the method chosen, it is also feasible and easy to train for only a fraction of an epoch, by simply beginning a pass through the data but not completing it. Without variance reduction techniques, there is a strong possibility that high-weight data points would be missed if a whole pass through the data is not done, however either of the two variance-reduction techniques presented here resolve this potential issue.

### A.3 Implementation of Weighted Training

One of the benefits of weighted retraining which we would like to highlight is its ease of implementation. Below, we give example implementations using common machine learning libraries.

#### A.3.1 PyTorch

##### Standard Training

```
criterion = nn.MSELoss()
outputs = model(inputs)
loss = criterion(outputs, targets)

loss.backward()
```

##### Weighted Training

```
criterion = nn.MSELoss(reduction=None)
outputs = model(inputs)
loss = criterion(outputs, targets)
loss = torch.mean(loss * weights)
loss.backward()
```

#### A.3.2 Keras

##### Standard Training

```
model.fit(x, y)
```

##### Weighted Training

```
model.fit(x, y, sample_weight=weights)
```

### A.4 Implementation of Rank Weighting

We provide a simple implementation of rank-weighting:

```
import numpy as np
def get_rank_weights(outputs, k):

    # argsort argsort to get ranks (a cool trick!)
    # assume here higher outputs are better
    outputs_argsort = np.argsort(-np.asarray(outputs))
    ranks = np.argsort(outputs_argsort)
    return 1 / (k * len(outputs) + ranks)
```

### A.5 Rank-Weighted Distributions of Objective Function Values of 2D Shape and Arithmetic Expression Datasets

Finally, to complement the rank-weighted distributions of objective function values of the ZINC dataset in Fig. 2, we here also show the corresponding distributions for the 2D shape and arithmetic expression datasets used in Sections 6.1 and 6.2, respectively.



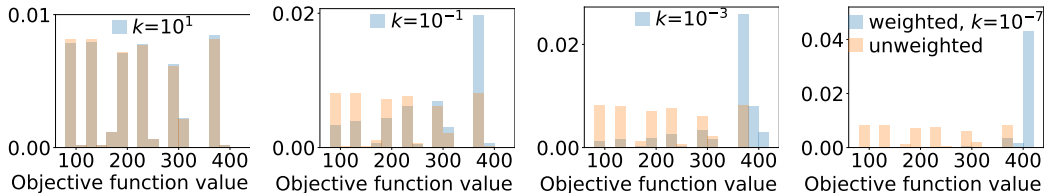


Figure 6: Distribution of objective function values of the 2D shape dataset (see Section 6.1), weighted uniformly (orange) and with the rank weighting in Eq. (3) (blue). Large  $k$  approaches uniform weighting, while small  $k$  place most weight on the best (i.e., largest) objective function values.

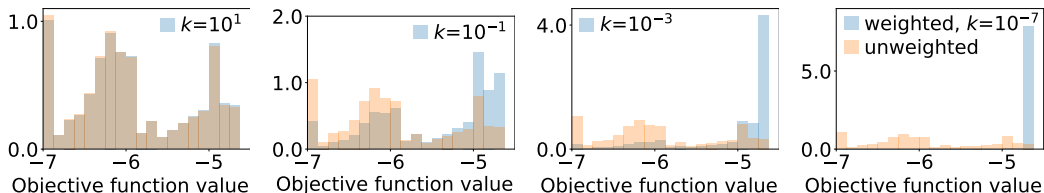


Figure 7: Distribution of objective function values of the arithmetic expression dataset (see Section 6.2), weighted uniformly (orange) and with the rank weighting in Eq. (3) (blue). Large  $k$  approaches uniform weighting, while small  $k$  place most weight on the best (i.e., largest) objective function values.

## B Further Experimental Results

### B.1 Area Distribution of Uniform Enumeration of Latent Space on the 2D Shape Task

Figure 3 (right) showed the distributions of shapes obtained from *sampling from the generative model’s prior*, supporting the hypothesis that weighted (re)training of the generative model changes the learned latent manifold to contain a larger fraction of high-performing points (which gets more pronounced with smaller values of  $k$ ). However, since samples from the generative model’s prior lie in regions with high probability mass under the prior and thus do not cover the entirety of the latent space, one might argue that Fig. 3 (right) does not serve as appropriate evidence for our hypothesis.

Therefore, in Fig. 8 we show the distributions of shapes obtained from *uniformly enumerating the feasible region of the model’s latent space*. In particular, as in Section 6.1, we evaluate all points lying on a uniformly-spaced grid in latent space within the  $\ell_2$ -ball of radius 5 (which is only tractable due to the low dimensionality of the learned latent space). Fig. 8 shows that the distributions of objective function values when enumerating the latent space roughly matches the distributions when sampling from the model’s prior shown in Fig. 3 (right). Fig. 8 thus confirms our hypothesis that lower  $k$  values do indeed lead to a significant change in the contents of the latent space, and that weighted (re)training creates new, high performing regions in latent space that do not exist in unweighted training.

### B.2 Top10 and Top50 Plots for Arithmetic Expression Fitting and Chemical Design Tasks

Fig. 9 shows results on the arithmetic expression fitting and chemical design tasks from Sections 6.2 and 6.3, reporting Top10 and Top50 scores, to complement the Top1 scores shown in Fig. 4. As a continuation of Fig. 4, which showed the Top1 score for the Arithmetic Expression Fitting and Chemical Design tasks, Fig. 9 shows the Top10 and Top50 scores. Weighted retraining also outperforms all other methods on these metrics, showing that weighted retraining is able to reliably discover *many* high-scoring points, while other methods perform significantly worse.

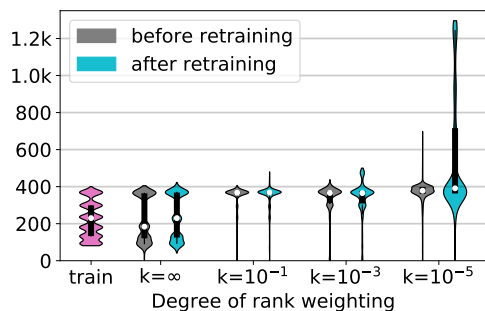


Figure 8: Distributions of areas of shapes from the training set, and of shapes obtained from uniformly enumerating the latent space, for  $k \in [\infty, 10^{-1}, 10^{-3}, 10^{-5}]$ .

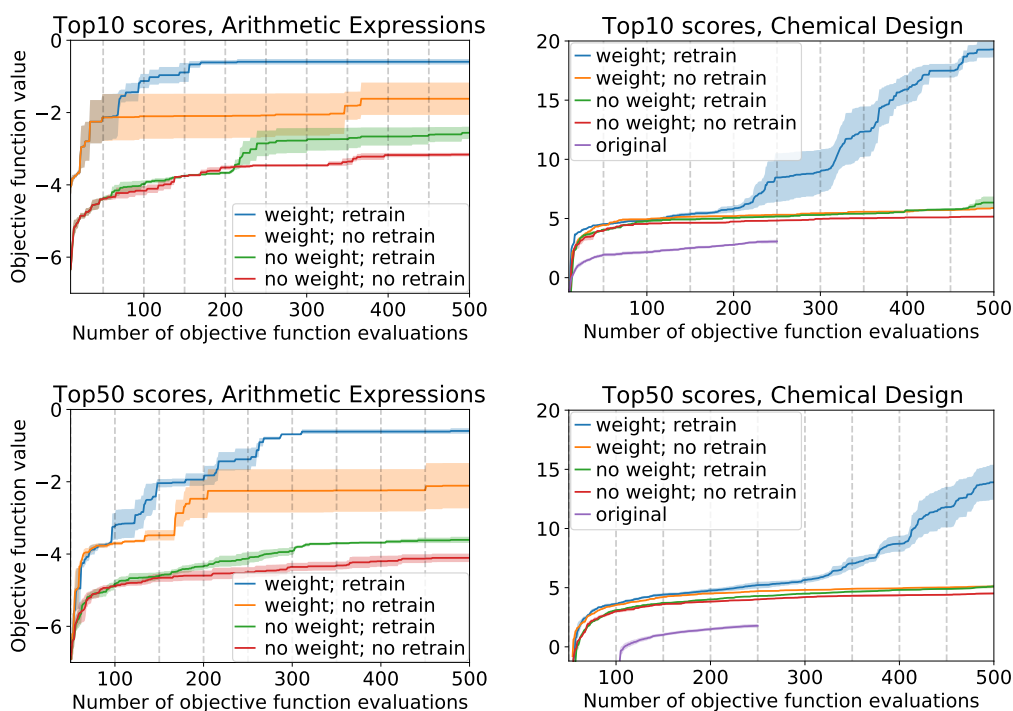


Figure 9: Mean  $\pm$  one standard error (over 3 random seeds) of the Top10 scores (top row) and Top50 scores (bottom row) on the arithmetic expression fitting task (left column) and the chemical design task (right column), using rank weighting with  $k = 10^{-3}$ . (Right) The purple line labelled “original” shows the results from [21], extracted from their GitHub repository. Weighted retraining achieves significantly better optimization performance and higher sample efficiency than the baselines on both tasks, and in particular on the chemical design task.

### B.3 Objective Function Value Distribution for Prior Samples on the Chemical Design Task

We consider a series of weighted models with different  $k$  values obtained by fine-tuning the pre-trained model used in Section 6.3 on the weighted training objective for 1 epoch each. To measure the effect of this fine-tuning, we sampled from the prior of each of these models, and calculated the objective function values of the samples. The resulting distributions are plotted in Fig. 10, which shows a clear shift towards higher scores as  $k$  decreases. This suggests that the feasible region of the latent space had been successfully modified to consist of a much higher fraction of high-performing points compared to the original model.

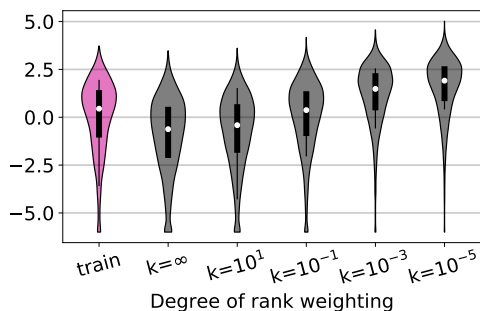


Figure 10: Distributions of objective function values of molecules from the training set, and of molecules sampled from the generative model’s prior (before retraining), for  $k \in [\infty, 10^1, 10^{-1}, 10^{-3}, 10^{-5}]$ . The distributions clearly shift towards higher objective function values for smaller  $k$ . Compare this also to Fig. 2, which shows the weighted training data distributions.

#### B.4 Plots for Different Degrees of Rank Weighting on the Chemical Design Task

Fig. 11 shows the results of an ablation study in which all parameters are held fixed and only the parameter  $k$  that controls the degree of rank weighting is varied.

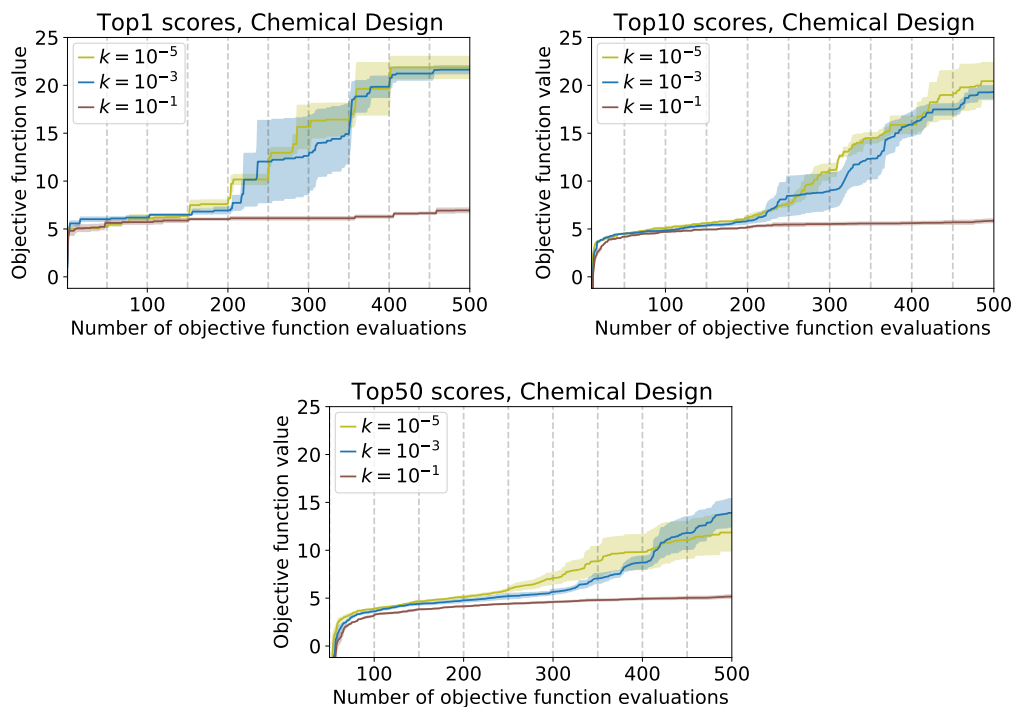


Figure 11: Mean  $\pm$  one standard error (over 3 random seeds) of the Top1, Top10 and Top50 scores of weighted retraining on the chemical design task, using rank weighting for different values of  $k$ , i.e.  $k \in [10^{-1}, 10^{-3}, 10^{-5}]$ . While the performance is almost identical for  $k = 10^{-3}$  and  $k = 10^{-5}$ , it is significantly worse for  $k = 10^{-1}$ , showing the importance of having a weighting distribution that is not too close to the uniform distribution. See Figs. 2 and 10 for visualizations of the weighted objective function value distribution for  $k = 10^{-1}$ .

## B.5 Comparison of Chemical Design Results with Previous Papers

Table 1 compares the results attained in this paper with the results from previous papers that attempted the same task. Weighted retraining clearly beats the previous best methods, which were based on reinforcement learning, while simultaneously being more sample-efficient.

Model	1st	2nd	3rd	no. queries (source)
JT-VAE [21]	5.30	4.93	4.49	2500 (paper <sup>5</sup> )
GCPN [64]	7.98	7.85	7.80	$\approx 10^6$ (email <sup>6</sup> )
MolDQN [65]	11.84	11.84	11.82	$\geq 5000$ (paper <sup>7</sup> )
<b>JT-VAE</b> (our Bayesian optimization)	5.46	5.44	5.28	500
<b>JT-VAE</b> ( $k = 10^{-3}$ , no retraining)	6.72	6.31	6.10	500
<b>JT-VAE</b> ( $k = 10^{-3}$ , retraining)	20.80	20.64	20.27	500
<b>JT-VAE</b> ( $k = 10^{-3}$ , retraining, <i>best result</i> )	<b>22.55</b>	<b>21.75</b>	<b>21.30</b>	<b>500</b>

Table 1: Comparison of top 3 scores on chemical design task. Baseline results are copied from [65]. All our results state the *worst* of 3 runs (unless otherwise stated), each run being 500 epochs.

## B.6 Pictures of the Best Molecules Found by Weighted Retraining

Figure 12 illustrates some of the best molecules found with weighted retraining. Note that all the high-scoring molecules are extremely large. It has been reported previously that larger molecules achieve higher scores, thereby diminishing the value of this particular design task for RL algorithms [65]. However, the fact that these molecules were found with a generative model strongly highlights the ability of weighted retraining to find solutions outside of the original training distribution.

## C Details on Experimental Setup

### C.1 Weighting and Retraining

For weighting the data, we use the rank-based weighting function defined in Eq. (3), with  $k = 0.001$  (if not specified otherwise), which we found to be robustly working well across all the tasks we considered. We consider a budget of  $B = 500$  function evaluations, which is double the budget used in [29, 21]. For the settings in which we retrain the generative model, we do so after every 50th function evaluation (thus resulting in retraining the model nine times in total: after iterations 50, 100, . . . , 400 and 450), and use we fine-tuning (i.e., training on top of the previous model) rather than full retraining from scratch for efficiency.

### C.2 Bayesian Optimization

For optimizing over the latent manifold, we follow previous work [29, 21] and use Bayesian optimization with a variational sparse Gaussian process (SGP) surrogate model [56] (with 500 inducing points) and the expected improvement acquisition function [23]. We re-implemented the outdated and inefficient Theano-based Bayesian optimization implementation of [29] (see <https://github.com/mkusner/grammarVAE>), which was also used by [21], using the popular and modern Tensorflow 2.0-based GPflow Gaussian process library [8] to benefit from GPU acceleration. Our code base will be uploaded to github at a future date.

For computational efficiency, we fit the SGP only on a subset of the data, consisting of the 2000 points with the highest objective function values, and 8000 randomly chosen points. This also has the effect of ensuring that the SGP properly fits the high-performing regions of the data. Disregarding computational efficiency, we nonetheless found that fitting on this data subset remarkably improved performance of the optimization, even using the baseline model (without weighted retraining).

<sup>5</sup>These were the top results across 10 seeds, with 250 queries performed per seed.

<sup>6</sup>Obtained through email correspondence with the authors.

<sup>7</sup>The experimental section states that the model was trained for 5000 episodes, so at least 5000 samples were needed. It is unclear if any batching was used, which would make the number of samples greater.

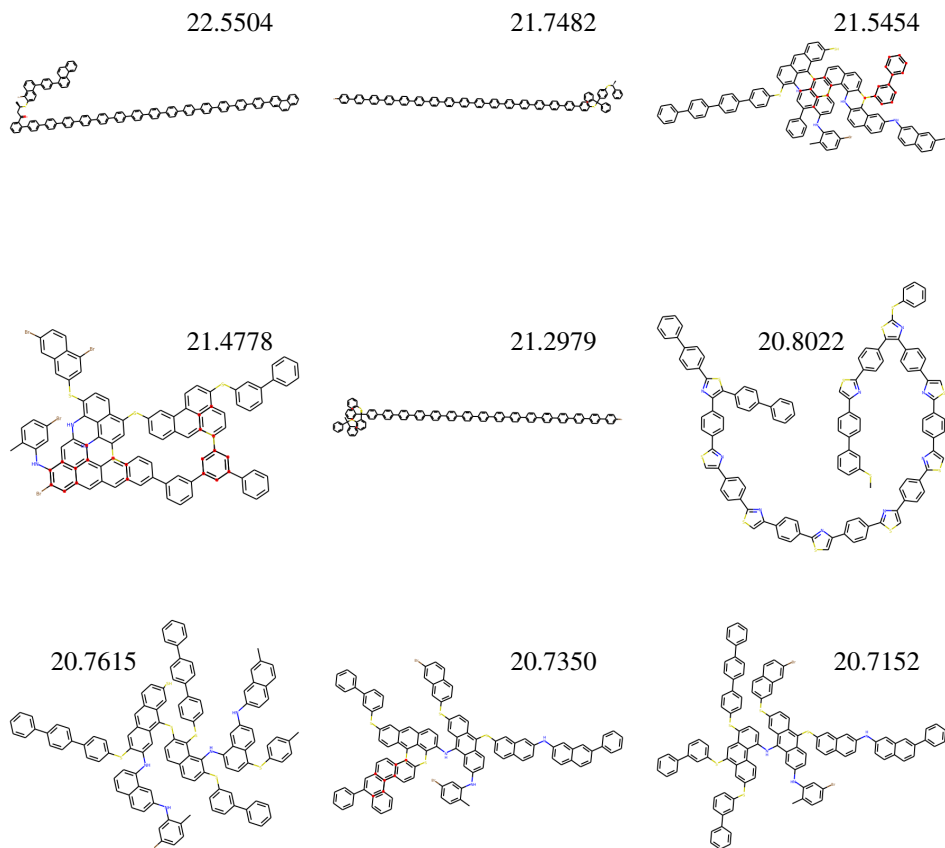


Figure 12: Some of the best molecules found using weighted retraining. Numbers indicate the score of each molecule.

### C.3 Evaluation Metrics

We report, as a function of the objective function evaluation  $b = 1, \dots, B$ , the single best score obtained up until query  $b$  (denoted as Top1), and the worst of the 10 and 50 best scores obtained up until evaluation query  $b$  (denoted as Top10 and Top50, respectively). Since our goal is to synthesize entities with the desired properties that are both a) *syntactically valid* and b) *novel*, we discard any suggested data points which are either a) invalid or b) contained in the training data set (i.e., they are not counted towards the evaluation budget and thus not shown in any of the plots). For statistical significance, we always report the mean plus/minus one standard error across three random seeds.

### C.4 2D Shape Task

Fig. 13 shows example images sampled uniformly at random from the subset of the dSprites dataset we use for the 2D shape task, comprising of squares with different sizes, positions and rotations.

As the generative model, we use a convolutional VAE architecture with a 5-dimensional latent space, which we found to be sufficient for modeling this rather simple dataset. The encoder consists of three convolutional layers with 32, 64 and 128 channels, respectively, and with a stride of 2 and a kernel size of 5, followed by two fully-connected layers with 4096 and 1024 units, respectively. The decoder has the same architecture as the encoder but mirrored, using transposed convolutions instead of convolutions (ConvTranspose2d in PyTorch). We use rectified linear units as the non-linear

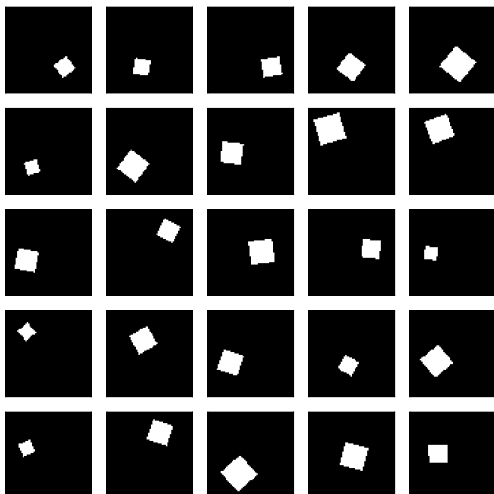


Figure 13: Example images sampled uniformly at random from the dataset of 2D shapes we use.

transformation between the layers. Following general conventions, we use a standard normal prior  $p(\mathbf{z}) = \mathcal{N}(0, 1)$  over the latent variables  $\mathbf{z}$  and a Bernoulli likelihood  $p(\mathbf{x}|\mathbf{z})$  to sample binary images.

### C.5 Arithmetic Expression Fitting Task

Following [29], the dataset we use consists of randomly generated univariate arithmetic expressions from the following grammar:

$$\begin{aligned} S &\rightarrow S '+' T \mid S '*' T \mid S '/' T \mid T \\ T &\rightarrow '(' S ')' \mid '\sin(' S ')'\mid '\exp(' S ')'\mid \\ T &\rightarrow 'v' \mid '1' \mid '2' \mid '3' \end{aligned}$$

where  $S$  and  $T$  denote non-terminals and the symbol  $|$  separates the possible production rules generated from each non-terminal. Every string in the dataset was generated by applying at most 15 production rules, yielding arithmetic expressions such as  $\sin(2)$ ,  $v/(3+1)$  and  $v/2 * \exp(v)/\sin(2*v)$ , which are all considered to be functions of the variable  $v$ .

The objective function we use is defined as  $f(\mathbf{x}) = -\log(1 + \text{MSE}(\mathbf{x}, \mathbf{x}^*))$ , where  $\text{MSE}(\mathbf{x}, \mathbf{x}^*)$  denotes the mean squared error between  $\mathbf{x}$  and the target expression  $\mathbf{x}^* = 1/3 * v * \sin(v*v)$ , computed over 1000 evenly-spaced values of  $v$  in the interval between  $-10$  and  $+10$ . We apply the logarithm function following [29] to avoid extremely large MSE values resulting from exponential functions in the generated arithmetic expressions. In contrast to [29], we negate the logarithm to arrive at a maximization problem (instead of a minimization problem), to be consistent with our problem formulation and the other experiments. The global maximum of this objective function is  $f(\mathbf{x}) = 0$ , achieved at  $\mathbf{x} = \mathbf{x}^*$  (and  $f(\mathbf{x}) < 0$  otherwise).

In contrast to the original dataset of size 100,000 used by [29], which *includes the target expression* and many other well-performing inputs (thus making the optimization problem easy in theory), we make the task more challenging by discarding the 50% of points with the highest scores, resulting in a dataset of size 50,000 with objective function value distribution shown in Fig. 7.

We use the original implementation of the grammar VAE of [29] provided at <https://github.com/mkusner/grammarVAE>, which we minimally modify to include weighted retraining.

### C.6 Chemical Design Task

The precise scoring function for a chemical  $\mathbf{x}$  is defined as  $\text{score}(\mathbf{x}) = \max(\widehat{\log P(\mathbf{x})} - \widehat{\text{SA}(\mathbf{x})} - \widehat{\text{cycle}(\mathbf{x})}, -6)$ , where  $\log P$ ,  $\text{SA}$ , and  $\text{cycle}$  are property functions, and the  $\widehat{\phantom{x}}$  operation indicates standard normalization of the raw function output using the ZINC

training set data (i.e. subtracting the mean of the training set, and dividing by the standard deviation). This is identical to the scoring function from references [29, 5, 21, 65, 64], except that we bound the score below by  $-6$  to prevent points with highly-negative scores from substantially impacting the optimization procedure. Functionally, because this is a maximization task, this makes little difference to the scoring of the outcomes, but does substantially help the optimization.

### C.7 Other Reproducibility Details

**Range of hyperparameters considered** We considered  $k$  values in the range  $10^1, 10^0, \dots, 10^{-5}$ , and found that there was generally a regime where improvement was minimal, but below a certain  $k$  value there was significant improvement (which is consistent with our theory). We chose  $k = 10^{-3}$  as an intermediate value that consistently gave good performance across tasks. This value was chosen in advance of running our final experiments (i.e. we had preliminary but incomplete results with other  $k$  values, then chose  $k = 10^{-3}$ , and then got our main results). The hyperparameters for model design and learning were dictated by the papers whose models we chose, except for the convolutional neural network for the shape task, where we chose a generic architecture.

**Average runtime for each result** All experiments were performed using a single GPU. Runtime results are given in Table 2.

Experiment	GPU hours per run	Number of runs
Shapes (model pre-training)	36:00	2 (1 weighted, 1 unweighted)
Shapes (optim., retraining)	03:30	2 (1 weighted, 1 unweighted)
Shapes (optim., no retraining)	00:02	2 (1 weighted, 1 unweighted)
Expressions (model pre-training)	12:00	2 (1 weighted, 1 unweighted)
Expressions (optim., retraining)	04:15	6 (3 weighted, 3 unweighted)
Expressions (optim., no retraining)	02:45	6 (3 weighted, 3 unweighted)
Chemical Design (retraining)	20:00	6 (3 weighted, 3 unweighted)
Chemical Design (no retraining)	03:00	6 (3 weighted, 3 unweighted)

Table 2: Approximate runtimes of main experiments

**Computing infrastructure used** All experiments were done using a single GPU (either NVIDIA P100, 2070 Ti, or 1080 Ti). In practice, a lot of the experiments were run on a high-performance computing cluster to allow multiple experiments to be run in parallel, although this was strictly for convenience: in principle, all experiments could be done on a single machine with one GPU.